

Observations of elves and radio wave perturbations by lightning

Maja Tomicic¹, Olivier Chanrion¹, Thomas Farges², Janusz Mlynarczyk³,
Ivana Kolmašová^{4,5}, Serge Soula⁶, Christoph Köhn¹, Torsten Neubert¹

¹DTU Space, Technical University of Denmark, Lyngby, Denmark

²CEA, DAM, DIF, F-91297, Arpajon, France

³Institute of Electronics, AGH University of Science and Technology, Krakow, Poland

⁴Department of Space Physics, Institute of Atmospheric Physics, Czech Academy of Sciences, Prague,
Czech Republic

⁵Faculty of Mathematics and Physics, Charles University, Prague, Czech Republic

⁶Laboratoire d'Aérodynamique, Université de Toulouse, UT3, CNRS, IRD, Toulouse, France

Key Points:

- Analysis of 63 elves above a thunderstorm in the Adriatic Sea and perturbations to MF and/or VLF transmitter signals passing the storm
- Lightning causing elves has \sim ten times the power and \sim three times the iCMC of lightning with a similar peak current without elves
- Only LOREs are observed with elves. Shorter VLF perturbations are likely caused by e-field driven electron attachment in the mesosphere

Corresponding author: Maja Tomicic, majtom@space.dtu.dk

19 **Abstract**

20 The electromagnetic and electrostatic fields from powerful lightning heat and ionize the
 21 lower ionosphere. The disturbances appear as halos, sprites and elves, and are also ob-
 22 served as perturbations in crossing radio signals. The characteristic of the lightning dis-
 23 charges leading to the various types of perturbations is not fully understood. Here we
 24 present an analysis of 63 elves and corresponding VLF and MF signal perturbations from
 25 an almost stationary thunderstorm that allows us to untangle some of the dependencies
 26 of perturbations on the lightning characteristics. We characterize the perturbations to
 27 a VLF-transmitter signal as "long-recovery-early-events" (LOREs), "early" events, or
 28 "rapid-onset-rapid-decay" (RORD) events. We find that LOREs are related to high light-
 29 ning current and bright elves, and their amplitude and sign depend on their location along
 30 the signal path. With observations in the ELF and MF band, we find that lightning with
 31 elves has three times the impulse charge moment change (iCMC) and ten times the power
 32 than lightning of similar peak current without elves. Attenuation in MF links appear in
 33 a higher proportion and longer duration observed with elves than with high peak cur-
 34 rent lightning without elves. The remaining types of VLF perturbations occur without
 35 TLEs but with sequences of lightning that produce slowly rising CMCs reaching high
 36 values (up to ~ 3500 C km within ~ 500 ms). Slower rise times lead to lower fields in the
 37 mesosphere that may not create significant ionization but instead drive dissociative at-
 38 tachment of free electrons. The depletions can result in perturbations to crossing VLF
 39 signals.

40 **Plain Language Summary**

41 Powerful lightning can create local disturbances to the atmosphere at around 70-
 42 100 km altitude. Such disturbances appear as phenomena known as halos, sprites and
 43 elves and can also be observed as changes in phase and amplitude of radio communica-
 44 tion signals that pass through the disturbed region. The characteristics of the lightning
 45 strokes leading to the various types of perturbations is not fully understood. In this work,
 46 we analyse 63 elves and corresponding amplitude changes in radio signals from an al-
 47 most stationary thunderstorm that allows us to untangle some of the dependencies of
 48 perturbations on the lightning characteristics. We find that lightning that produce elves
 49 has ten times the power and three times the impulse charge moment change than light-
 50 ning of similar peak current that did not produce elves. Also we find that elves are as-
 51 sociated with the longest types of perturbations (~ 10 min duration) in the VLF radio
 52 signals, whereas the shorter types of perturbations (~ 1 min duration) occur without op-
 53 tical emission. Our results suggests that these are a result of density changes at 70-85
 54 km altitude caused by electron attachment by slower rising electric fields.

1 Introduction

Elves are rings of optical emissions at the base of the ionosphere ($\sim 80\text{-}95$ km altitude) that expand rapidly up to ~ 700 km diameter during ~ 1 ms following a powerful cloud-to-ground (CG) lightning stroke. They are emissions from atmospheric constituents that are excited and ionized by collisions with free electrons heated by the electromagnetic pulse (EMP) radiated by the lightning return current (Fukunishi et al., 1996; Barrington-Leigh & Inan, 1999; van der Velde & Montanyà, 2016). Since their first discovery from the space shuttle orbiters (Boeck et al., 1992), elves have been studied from the ground (e.g., Fukunishi et al., 1996; Blaes et al., 2016; van der Velde & Montanyà, 2016; Kolmašová et al., 2021), from space (e.g., Chen et al., 2008, 2014) and with models (e.g., Inan, Sampson, & Taranenko, 1996; Marshall et al., 2010; Marshall, 2012). The properties of lightning return strokes that control the excitation of elve emissions are still not fully understood because comprehensive data are lacking caused, for instance, by limitations in instrument sensor sensitivities, triggered data selection, and the relatively modest number of optical observations of elves. Whereas the radiated EMP is proportional to the time derivative of the peak current, the most commonly adopted parameter for elve probability is the peak current itself because it is a parameter provided by lightning detection networks. An estimate of the lower limit required to generate elves range from ~ 38 kA (Chen et al., 2014), where elves were observed with the ISUAL spectrophotometer from space, to ~ 130 kA (van der Velde & Montanyà, 2016) based on camera observations from ground in Spain and France. Observations in the western United States concluded that the threshold for 50% probability of elves was 88 kA and 90% probability at 106 kA (Blaes et al., 2016). Global variations in the height of the ionosphere and electron density gradients with altitude may influence the production of elves, as well as meteorological variations such as thunderstorm altitudes, and thereby the average lightning channel length (Blaes et al., 2016). Thus, van der Velde and Montanyà (2016) found elves far more likely in maritime winter thunderstorms than summer thunderstorms over land and Chen et al. (2014) found only dependence on stroke energy, but no significant oceanic and land difference. The diversity of conditions in the above reports points to the difficulty in determining a globally and seasonally independent lower limit on peak current (or other lightning parameters) for the causative lightning of elves.

Narrow-band navigational transmitter signals in the VLF band propagate in the earth-ionosphere wave-guide. They reflect at altitudes of elves and the signal properties are therefore affected by conductivity changes at this boundary. The electron density changes associated with elves (Marshall et al., 2010) cause steplike perturbations to the transmitter signals (amplitude and phase) if the transmitter-receiver (TR) path crosses the region affected by the elve. Such perturbations are called Long Recovery Early Events (LOREs) (e.g., Haldoupis et al., 2013; Mika et al., 2006; Naitamor et al., 2013; Salut et al., 2012). They fall into the category of "early" VLF events because they are caused by direct coupling of the lightning EMP and the ionosphere, thus showing a very short delay (a few ms) from the return stroke pulse. LOREs persist for tens of minutes, and sometimes the signal does not recover before it is masked by other variations in the signal levels (Mika et al., 2006). The long recovery time is linked to the lifetime of free electrons at this altitude (Rodger, 2003). The LORE phenomenon has almost exclusively been observed in association with elves and is considered the VLF signature of elves (Haldoupis et al., 2013; Mika et al., 2006; Kolmašová et al., 2021), although larger data sets have not been published until now. On the other hand, the physical mechanisms responsible for "early/fast" and "early/slow" VLF events (Inan et al., 1993; Haldoupis et al., 2006), which are similar to LOREs but with recovery within a few minutes, are still under debate (Marshall et al., 2008; Kabirzadeh et al., 2017). They relate to sprites (Inan et al., 1995; Haldoupis et al., 2004, 2010) and sprite halos (Moore et al., 2003); however, numerous observations of early/fast events with no associated transient luminous events (TLEs) also exist (Marshall et al., 2006). To relate to sprites and halos they must be driven by the quasi-electrostatic (QE) field of lightning discharges. The field affects the atmo-

sphere at lower altitudes (70-80 km) where the lifetimes of free electrons are of the order of 10-100 s (Pasko & Inan, 1994; Rodger et al., 1998) in line with the observed recovery rates. Another type of VLF perturbation associated with the QE field of lightning are the so-called "rapid onset rapid decay" (RORD) events (Dowden et al., 1994; Inan, Slingeland, et al., 1996). With onsets within 20 ms and recovery in less than 3 seconds, corresponding to the duration of the field, they are believed to be VLF signatures of the conductivity changes due to heating by QE fields (Inan, Slingeland, et al., 1996).

Narrow-band signals from radio transmitters in the MF band (0.3-3 MHz) reflect during the nighttime at ~ 105 km altitude and may be absorbed if passing through disturbed regions. Strong CG strokes are found to be associated with ms-duration attenuation of narrow-band radio transmission in a band of 500 - 1600 kHz, with the amplitude of attenuation proportional to the peak current of the causative stroke (Farges et al., 2007). Although MF perturbations are four-five orders of magnitude shorter than VLF perturbations, the size of the perturbed regions is comparable. To understand this brief blackout phenomenon, Farges et al. (2007) modeled the propagation of the MF radio waves through a region of the ionosphere disturbed by the lightning EMP under three different scenarios: that the EMP causes only ionization, only electron heating, and both combined. The results were compared to the absorption calculations obtained in the absence of flashes and showed that electron heating alone could explain the measured attenuation. Moreover, the decay of electron heating, which is less than 100 ms at elve altitudes (Rodger et al., 1998), is the only process that is compatible with the observed attenuation (1 - 10 ms). For comparison, the decay of enhanced ionization is 10,000 times longer. Finally, Farges et al. (2007) concluded that the disturbances could be an additional signature of the presence of elves. However, simultaneous observations of elves and MF blackouts have not been published until now.

In this paper, we present observations of a high number of elves produced over the Adriatic Sea during the night of December 9-10, 2020, with simultaneous observations of perturbations in the signals of one VLF link and seven MF links passing the region. Our goal is to investigate the relationship between lightning characteristics and lightning effects in the ionosphere. For the first time (to our knowledge), optical observations of 63 elves were recorded from an almost stationary storm. The observations offer a rare opportunity to limit the influence of geographic location, local time and season, viewing conditions and instrument sensitivity while still having a large data sample. We include in our analysis impulse current moment changes (iCMC) and charge moment changes (CMC) of selected strokes derived from Extremely Low Frequency (ELF) measurements and energy of causative strokes from broadband electric field measurements. The relationship between the LOREs of positive and negative polarity is discussed from perturbations by a second storm on the Italian south coast towards the Tyrrhenian Sea.

2 Data, instrumentation and methods

2.1 Lightning data

We use lightning data from the Vaisala Global Lightning Dataset, GLD360 (Said et al., 2010; Said & Murphy, 2016). It contains time, location, peak current and type (CG or intracloud (IC)). The detection efficiency (DE) and location accuracy (LA) in the USA is evaluated to $\sim 75-85\%$ relative to the National Lightning Detection Network, which has a flash DE $>95\%$ (Mallick et al., 2014). The median LA is 1.8 km. The accuracy in the Adriatic sea is assumed to be the same, as the sensor density is similar to that in the USA (R. Said, personal communication, March 17, 2021).

The vertical broadband electric field from 1 kHz to 5 MHz was measured with a dipole whip antenna installed in the center of France, 900 to 1050 km from the storm location (labelled "BB" in Figure 1) (Farges & Blanc, 2011). The system triggers if the

159 field exceeds 2 V/m, storing 30 ms of data from 6 ms before the trigger at a sampling
 160 frequency of 12.5 MHz. We use the measurements to characterize lightning and black-
 161 outs of MF radio transmitter signals.

162 The current moment waveform (CMW) and CMC were obtained from measure-
 163 ments of an ELF receiver system in the Bieszczady mountains in Poland (49.2°N, 22.5°E
 164 ~850 km from the storm and labelled "ELF" in Figure 1). It measures the magnetic field
 165 component with two antennas aligned in the north-south and east-west directions in the
 166 frequency range 0.02 Hz to 1.1 kHz. The receiver features a Bessel anti-aliasing filter with
 167 a bandwidth of 900 Hz. The sampling frequency is 3 kHz. The CMW and the CMC were
 168 reconstructed using the method of Mlynarczyk et al. (2015) that accounts for the depen-
 169 dence with the frequency of the signal attenuation and the propagation velocity in the
 170 ELF range.

171 2.2 VLF receiver

172 A Sudden Ionospheric Disturbances (SID) monitor measures perturbations to narrow-
 173 band VLF signals from powerful transmitters used for communication with submarines.
 174 The monitor used in this study is operated by the Slovak Organization for Space Activ-
 175 ities and placed in Bojnice, Slovakia (48.8°N, 18.6 °, labelled "SID" in Figure 1). It can
 176 record up to sixteen VLF transmitters simultaneously with a sampling frequency of 2
 177 Hz. We use the NSY transmitter operated by the Naval Computer and Telecommuni-
 178 cations Station in Sicily (37.1°N, 14.4°E), which broadcasts at 45.9 kHz with 250 kW.
 179 The signal propagates from Sicily to Slovakia (~1345 km) and reflects multiple times at
 180 the surface of the Earth and the bottom of the ionosphere. The propagation great circle
 181 path (GCP) of the NSY signal crosses directly the thunderstorm location (see Fig-
 182 ure 1).

183 2.3 Optical observations

184 The optical observations are performed by a TLE observatory installed in Rustrel,
 185 France (43.94° N, 5.48° E) at 1025 m altitude. It is mounted on a building made avail-
 186 able by Laboratoire Souterrain à Bas Bruit (LSBB). The camera is a Watec 1/2" monochrome
 187 CCD camera (WAT-902H) with a 16 mm lens that gives ~23° horizontal and 17° ver-
 188 tical field of view (FOV). It takes 50 interlaced fields per second, corresponding to a time
 189 resolution of 20 ms. The images are time referenced after synchronization with an NTP
 190 server, giving an absolute time uncertainty below 5 ms. The camera is mounted on a Quick-
 191 Set motorized Pan-Tilt unit allowing for active and automatic tracking of thunderstorms.
 192 The night of the observations, the camera tracked two thunderstorms automatically, se-
 193 lecting a new pointing direction every 15 minutes. The camera, therefore, pointed away
 194 from the storm during parts of the night. The analysis excludes strokes that occurred
 195 in these gaps. From 02:45 UTC the camera stayed in the same position for the rest of
 196 the night.

197 2.3.1 Methods and error estimations

198 Figure 2, shows an image of an elve that occurred at 03:57:56.578 UTC on Decem-
 199 ber 10th, 2020. From the images, we estimated their altitude and relative brightness. Fol-
 200 lowing van der Velde and Montanyà (2016), we calculated the altitude by combining the
 201 elevation of the elve centers retrieved from the software 'Cartes du ciel' with the loca-
 202 tion of the CG stroke reported by GLD360, assuming a spherical earth with radius of
 203 6370 km and a camera altitude of 1025 m. Before the image analysis, the background
 204 for each elve, determined as the mean value of two interlaced fields preceding the elve,
 205 was subtracted. The same fields were used to determine the elevation angle of the FOV.
 206 The elves are faint and diffuse, and their centers can be difficult to determine, which in-
 207 troduces an error in the elevation angle. We found that the read-out error was less than

0.1 deg, which corresponds to an altitude uncertainty of ± 1.4 km at 800 km distance to the elves. The uncertainty in the location of the parent strokes (median value 1.8 km (Said & Murphy, 2016)) introduces an uncertainty of around 0.3 km at 800 km distance to the storm. We estimated the relative brightness of the elves from the sum of all pixels in the background subtracted elve images after scaling by the size of the elve in the image. The brightest elve was used as a reference.

3 Meteorology and storm development

On December 9, 2020, a low-pressure system was centered over northern Italy according to the geopotential at 500 hPa with a minimum of about 5.275 km (red lines in Figure 1). The counter-clockwise winds reached up to 40 m s^{-1} at 500 hPa (~ 5.5 km), corresponding to large geopotential gradients along an arc extending over northern Africa and southern Italy. This jet carried warm, humid air from the Mediterranean Sea into the Adriatic Sea, enhancing strong atmospheric forcing in the region. Over the Adriatic Sea, the wind shear between 1000 and 500 hPa (0-5.5 km) was modest, and the CAPE was moderate ($< 700 \text{ J kg}^{-1}$) and higher over water. These conditions led to several electrically active cells that produced lightning with very high peak currents. Figure 3 shows the cloud top temperature (CTT) in the Adriatic Sea where the elves were observed (rectangle in Figure 1). The CTT is obtained from the $10.8 \mu\text{m}$ band of the Spinning Enhanced Visible and InfraRed Imager (SEVIRI) on the Meteosat Second Generation (MSG) satellite and is shown here for each hour of elve observation (20:00 UTC to 05:00 UTC). The CTT data is corrected for parallax, corresponding to 0.1° in latitude and 0.03° in longitude for cloud tops at ~ 10 km altitude. All CG strokes with peak currents above 200 kA absolute value are plotted with black crosses, and the elve-producing strokes are plotted in green. The elve-producing cells are less than 100 km across at $\text{CTT} < -40^\circ\text{C}$ (blue regions in Figure 3). The coldest CTT is about -60°C , which is not much colder than the tropopause (-56°C) at the same location, suggesting the clouds did not reach much above the tropopause. The elves were caused by strokes over the Adriatic Sea, where CAPE was higher than over land. In the second active region in southern Italy, more CG strokes are over land or at the coastline where CAPE in this region is higher (Figure 1). The CG stroke rate of the Adriatic storm does not exceed 10 CG strokes per minute. The relatively low convective activity, seen from the modest development of clouds cells and low stroke rate, is due to the limited CAPE and wind shear over the Adriatic Sea. From GLD360 we also get that 91% of the CG strokes produced in the Adriatic region (gray rectangle in Figure 1) from 19 to 6 UTC were negative with high average peak currents at -92 kA. The elve-producing strokes all have absolute peak currents stronger than 228 kA with an average of 453 kA.

4 Observations

4.1 Elves

During the night of the storm, the camera at Rustrel detected 63 elves. One is shown in Figure 2, and the rest is in the Figures S1-S63 in the Supporting Information. The lowest altitude at the storm that the camera could observe was 50 km (at 750 km distance) and 80 km (at 950 km distance). Thus, we cannot rule out other TLEs, such as sprites and halos, occurring below these altitudes. The camera observed the storm from 20:00 to 05:35 UTC with gaps totaling one hour and 45 minutes (22:00-22:30; 23:30-00:00; 00:30-01:15 UTC).

The optical characteristics were studied for all but a few elves. In four cases, no parent stroke was reported by GLD360 that allowed the estimation of their distance, three were too faint to define their shape, and the brightness of four could not be determined because the moon was behind the elve in the video field. Out of 63 elves, 56 were used for the brightness and altitude calculation.

258 The altitudes of the elves ranged from 80-90 km, which is within the range and vari-
 259 ability of the results in van der Velde and Montanyà (2016). All elves below 83 km oc-
 260 curred in the first hour of observations. We attribute this to the storm cell that was ac-
 261 tive during this hour rather than to changes in the ionosphere based on results from the
 262 NASA international reference ionosphere model (IRI). There is no clear trend between
 263 altitude and local time for the rest of the night. The relative brightness varies down to
 264 $\sim 17\%$ of the brightest elve. The brightness is correlated with the peak current and the
 265 Power Spectral Density (PSD) of the parent stroke in the band of the broadband receiver
 266 (see below), a parameter discussed in later paragraphs.

267 4.2 Lightning

268 During the periods the camera observed the storm, GLD360 detected 234 strokes
 269 with absolute values above 200 kA within the camera's FOV, leading to 175 of these that
 270 did not produce elves (CG strokes for four elves were not detected). To understand why
 271 some produced elves and others not, we made a parameter analysis of the waveform of
 272 the vertical electric field from the lightning strokes, measured by the broadband receiver
 273 in France. For each stroke, we determined the maximum amplitude of the ground wave
 274 (E_{GW}), the rise-time of the electric field pulse, defined as the time from 50% to 90% of
 275 E_{GW} , and the fall time from the maximum to the background. These statistics showed
 276 no apparent difference, a conclusion also reached when we averaged and compared the
 277 complete waveforms of those that generated elves with those that did not (see Figure
 278 S64 in the Supporting Information).

279 In Blaes et al. (2016), the peak current of the CG stroke is found to be a decisive
 280 parameter for elve generation, with a probability reaching 50% at 88 kA. Other authors
 281 found thresholds from 38 to 130 kA (Chen et al., 2014; van der Velde & Montanyà, 2016).
 282 In our case, the formation threshold of elves is around 200 kA. The variability of reported
 283 thresholds is likely an effect of the sensitivity of the optical instrument used (camera or
 284 photometer, for example), or uncertainty in the estimation of the peak currents reported
 285 by the detection networks. However, a question remains why not all high-current strokes
 286 generate elves, as noted in Kolmašová et al. (2021).

287 To explore this question further, we computed the electric field wave power, $P(E^2)$,
 288 which is the frequency integral of the electric field PSD over the whole antenna band-
 289 width (1 kHz to 5 MHz) using the method of Ripoll et al. (2021). It is computed over
 290 1.5 ms from the arrival time of the ground wave, to include the ground wave and all the
 291 sky waves. Figure 4 shows that the CG strokes producing elves have about one order of
 292 magnitude larger power, and also three orders of magnitude larger power than the typ-
 293 ical flashes analyzed in (Ripoll et al., 2021) using the same electric field sensor. This sug-
 294 gests that the generation of elves depends on the complete electromagnetic energy re-
 295 lease of the stroke.

296 We also analyzed ELF measurements of the electromagnetic signals from a subset
 297 of the lightning strokes from the sensor in the Bieszczady Mountains in Poland. The se-
 298 lection included high-current strokes with and without elves, and strokes with elves com-
 299 bined with no, weak or strong LOREs. We calculated the current moment (CM), the CMC
 300 and the impulse charge moment change (iCMC) (Cummer & Lyons, 2004) defined as the
 301 total CMC during the first 2 ms of the lightning stroke according to the method of Mlynarczyk
 302 et al. (2015). The iCMC is likely more relevant for elves than the total CMC since elves
 303 are generated within the first milliseconds. The results and other relevant stroke param-
 304 eters are presented in Table 1. We see that the iCMC and the CM are three times larger
 305 for strokes that generate elves. Larger values can result from larger currents, longer chan-
 306 nel lengths, or both. Since GLD360 data only provide the maximum current obtained
 307 in the VLF range, one cannot expect full correlation with the iCMC or CM, as pointed
 308 out in Lu et al. (2012). Their relation to LOREs is discussed in a following paragraph.

Table 1. Comparison of impulse charge moment change (iCMC) and current moment (CM) for strokes that produced elves, LOREs (strong or weak as sL or wL, respectively) or not. *reported polarities disagree.

Event	Time (UTC)	Lon (deg)	Lat (deg)	Peak current (kA)	iCMC (C km)	CM (kA km)
E + sL	12-09 20:09:08.217	15.46	43.39	-639	-133.2	-122
E + sL	12-09 22:48:54.353	16.56	42.90	-725	-148.5	-146
E + sL	12-10 01:33:38.668	15.68	43.09	-520	-146.6	-137
E + wL	12-09 23:05:50.076	16.67	42.97	-504	-106.5	-93
E	12-09 23:14:30.984	16.68	42.87	-535	-134.0	-120
E	12-10 01:16:58.561	14.84	42.81	-498	-117.4	-108
No E	12-10 20:25:15.397	15.27	43.34	+359*	-59.1	-55
No E	12-10 01:41:08.681	18.54	42.51	-430	-29.3	-33
No E	12-10 02:33:11.310	18.45	42.66	-378	-32.7	-30
No E	12-10 03:31:06.092	14.74	42.85	-426	-43.8	-39

309

4.3 VLF transmitter signal perturbations

310

311

312

313

314

315

316

317

318

319

320

321

322

323

324

325

326

327

328

The amplitude of the NSY VLF signal from the night of December 9-10th is shown in Figure 5 on different temporal scales. The variation on scales larger than ~ 30 minutes are not related to thunderstorm activity, but to other ionospheric processes because the signal from the same transmitter during a night without storms shows similar variations. However, amplitude perturbations on shorter scales are multiple, and many correlate in time with lightning activity detected by GLD360. These are identified using the criterion that the perturbation amplitude must be greater than 0.25 dB relative to the average amplitude (in dB) of the preceding 10 seconds. This condition corresponds to a threshold of 4σ , where σ is the average standard deviation for the night. The value is close to the typical value at 0.2 dB of Inan, Slingeland, et al. (1996). In addition, we require that a lightning stroke be detected by GLD360, or an elve by the camera, within 0.5 sec before the perturbation, corresponding to the temporal resolution of the receiver. The algorithm used to identify candidate events is used on a 3-point moving average of the signal, shown in Figure 6c in red. All candidate events are manually validated and categorized. The events are grouped in three categories: LOREs, the so-called "early/fast" or "early/slow" events (Inan et al., 1993; Haldoupis et al., 2006), and some events that are also early and fast but only last for 0.5-2 seconds, similar to the previously observed rapid onset, rapid decay (RORD) signatures (Dowden et al., 1994). In Figure 6 we show examples of the three types.

329

330

331

332

333

334

335

336

The time resolution of the VLF receiver (0.5 s) is sufficient to classify, with a high probability, events as "early" and to exclude lightning-induced electron precipitation that has onsets of 0.3-1.6 s relative to their causative stroke (Burgess, 1993; Peter & Inan, 2007). However, it does not allow for classification of the onset duration below 500 ms and therefore "early/fast" (onset < 20 ms) and "early/slow" fall in the same category, which we call "early" events (although, by definition LOREs and RORD are also early events). The origin of the "early/fast" and "early/slow" events is discussed in a later paragraph.

337

338

339

340

341

Based on their duration and shape, it is rather simple to categorize many perturbations as either LORE, "early" events, or RORD events. RORD events are simple because they only appear as short perturbations of 1-4 measurement points (2 Hz sampling frequency) before the signal returns to pre-lightning conditions. We identify 33 RORD events (3 with negative amplitude and 30 with positive amplitude of perturbation). Note

342 that the algorithm could miss some because the 3-point smoothing puts them below the
 343 0.25 dB threshold. The two other types are identified using a 20-point moving average
 344 (corresponding to 10 sec), and are shown in red in Figures 5 and 6a,b. "Early" events
 345 appear as sudden increases in the signal with a recovery (decrease of signal) that starts
 346 within 10 seconds of the peak. These events, therefore, appear as a peak with no plateau
 347 on the top in the smoothed signal. LOREs are defined as step-like perturbations that
 348 can be either positive or negative and that do not show recovery within the first 20 sec-
 349 onds. It means there will be either a plateau after the step or the amplitude keeps de-
 350 creasing/increasing for at least 20 sec (see the example in Figure 6a). We identify 68 "early"
 351 events (all with positive amplitude) and 18 LOREs (14 negative and 4 positive). The
 352 events are marked in Figure 5 and the main characteristics of the lightning strokes re-
 353 lated to the three types of perturbations are given in Table 2. There are also signal per-
 354 turbations related to high peak current lightning or even elves that have the shape of
 355 negative amplitude LOREs except that the onset is significantly slower at 1 to 3 s. One
 356 example is seen in Figure 5b at 22:46:53 UTC. For brevity, such events are not investi-
 357 gated further in this work.

358 Because of the considerable variation of the background signal and the high number
 359 of lightning-induced perturbations, it is hard to determine a recovery time for the
 360 individual perturbations. However, for all the "early" events, the recovery time looks shorter
 361 than 3 minutes (most are ~ 1 min), which is consistent with the typical recovery time
 362 of these events. The LOREs may not recover before other variations mask them. How-
 363 ever, they appear longer than the "early" events. In some cases, the perturbation is hard
 364 to categorize (positive LORE or "early" event) because the LORE step or the shape of
 365 an "early" event is unclear due to the varying background signal. Another complication
 366 is that perturbations can overlap. Thus, a few events can be miscategorized.

	LORE	"Early"	RORD
# of events (pos/neg amplitude)	18 (4/14)	68 (0/68)	33 (30/3)
Lightning peak current parameters in absolute value			
Range (kA) [min max]	[314 725]	[3 660]	[5 315]
# CG/IC	15/0*	49/19	31/2
# Neg/pos	14/1*	30/38	25/8
Mean/Median (kA)	526/526	82/45	124/107
95 % conf. int. (kA)	[461 592]	[55 108]	[94 154]

Table 2. Statistics from GLD360 data on the three types of VLF perturbations.

*Three events do not have parent lightning detected by GLD360, but coincide with elve.

367 Figure 7a,c shows the location of the lightning strokes related to the different types
 368 of perturbation and the histogram in Figure 7b shows the minimum distance from the
 369 stroke to the VLF path for all three types.

370 **4.3.1 LOREs**

371 13 out of 14 negative LOREs were associated with elves caused by lightning strokes
 372 of peak current ranging from 314 to 725 kA. The remaining negative LORE (at 23:36
 373 UTC) occurred simultaneously with a lightning stroke with a peak current of +536 kA
 374 when the camera was not observing the storm. Thus, it is likely that there was an elve
 375 at the time. These results show that the decreases considered as LOREs are related to
 376 elves. Nevertheless, the drop in the signal amplitude is counter to most reported LOREs

377 that exhibit a steep increase in amplitude, believed to be related to a better VLF sig-
 378 nal reflection efficiency (Haldoupis et al., 2013; Kolmašová et al., 2021). The four posi-
 379 tive LOREs were generated by the storm on the west coast of Italy, not covered by the
 380 camera. However, the related lightning strokes had high peak currents, ranging from -
 381 383 kA to -631 kA, making them very likely to produce elves. Therefore, we infer that
 382 a decrease or increase in the signal amplitudes is a signal propagation effect that depends
 383 on the relative locations of the transmitter, disturbance, and receiver, as proposed from
 384 observations and models (Haldoupis et al., 2013; Naitamor et al., 2013; Marshall & Inan,
 385 2010). As seen from Figure 5, most of the recorded elves (78%) were not associated with
 386 perturbations in the VLF signal, although they were caused by very high peak current
 387 lightning and occurred within 150 km from the VLF link. Also, the LOREs have very
 388 different amplitude. These observations will be discussed in Section 5.

389 **4.3.2 "Early" VLF events**

390 The "early" events, all seen as increases in the VLF signal, are unrelated to elves
 391 but correlate in time with lightning of both polarities within 150 km of the VLF path.
 392 The median of the absolute values of peak currents is 45 kA, and as seen from Table 2,
 393 this is much lower than for the LORE producing strokes and lower than the strokes re-
 394 lated to RORD events. The mean peak current and 95% confidence interval calculated
 395 for the "early" event strokes match the peak current intensities reported for this type
 396 of phenomenon earlier, e.g., 20 kA to 180 kA in Inan, Sampson, and Taranenko (1996).

397 We calculate the CMC for the discharges related to three of the "early" events (called
 398 a, b and c) and present the results in Table 3 together with the stroke parameters re-
 399 ported by GLD360. Figure 8 shows the current moment waveform and CMC for "early"
 400 event c. The three events are chosen because they are related to lightning from the same
 401 storm cell. Thus we limit the influence of differences in storm cell characteristics, re-
 402 lative location and local time. The time of the three events is read from Table 3 and the
 403 VLF signal perturbations are shown in Figure 5c. As seen from the example in Figure
 404 8, the CM waveform around the time of the event shows a series of discharges and con-
 405 tinuing current that make the CMC increase for almost 500 ms. All three "early" events
 406 studied here had similar signatures in ELF, and the CMC increased for at least 400 ms
 407 in all cases.

408 Some "early" events (19/68) coincide with IC discharges detected by GLD360 and
 409 without accompanying CG strokes. GLD360 reports peak current amplitudes for these
 410 IC discharges between 3 and 42 kA. We checked Earth Networks lightning data as well,
 411 and for 10 of these events, they also only report IC discharges. At the time of the remain-
 412 ing 9 events, Earth Networks reports either no lightning or a very low peak current (0.3
 413 to 7.5 kA) CG stroke. The locations of the IC discharges are marked with cyan stars in
 414 Figure 7c, and as seen here, all of them are located close (within 34 km) to the VLF path.
 415 In these cases, the lightning detection system could have missed the causative CG stroke.
 416 However, it is unlikely that two independent lightning detection networks both miss CG
 417 strokes but detect weak IC pulses. In addition, the similar location of the events sug-
 418 gests that they are, in fact, related to IC processes. Our interpretation aligns with Johnson
 419 and Inan (2000), who report on measurements of "early/fat" events without a parent
 420 CG but with spheric signatures interpreted as intracloud pulses, and many CG strokes
 421 with high currents close to the VLF signal path that were not associated with VLF events.
 422 They suggest that "early/fast" VLF events are exclusively produced by lightning episodes
 423 that include a large IC cluster. In addition, Haldoupis et al. (2006) note that the IC ac-
 424 tivity of weaker but densely clustered spherics can explain the slower onset of "early/slow"
 425 events that do not match the timescales of return strokes.

Table 3. Comparison of charge moment change (CMC) for discharges at the time of "early" and RORD events. The lightning stroke parameters (GLD360) are only shown for the strongest discharges, although weaker discharges were also detected in most cases. *reported polarities disagree.

Event	Time (UTC)	Lon (deg)	Lat (deg)	Peak current (kA)	CMC (C km)
"Early" event a	23:17:50.311	16.75	42.94	-26	854.1
"Early" event a	23:17:50.616	16.71	42.91	+68	2708.8
"Early" event b	23:29:57.844	16.72	42.87	-210	818.2
"Early" event b	23:29:57.988	16.73	42.90	+19	2876.6
"Early" event c	23:41:10.851	16.76	42.88	+51	3535.2
RORD a	22:53:17.210	16.61	42.96	-229	1374.0
RORD a	22:53:17.679	16.60	43.01	+53	1009.8
RORD b	23:01:25.721	16.67	42.94	-99	1160.5
RORD b	23:01:26.123	16.53	42.85	-39*	547.6
RORD c	23:02:19.6305	16.57	42.92	-33	1176.3

426

4.3.3 Rapid onset rapid decay events (RORD)

427

428

429

430

431

432

RORD events are believed to be VLF signatures of heating by QE fields in cases where the QE field is insufficient to drive ionization changes (Inan, Slingeland, et al., 1996). Heated electrons cool almost instantaneously, leading RORDs to last as long as the fields, typically less than a few seconds. In the storm, they are linked with lightning of both polarities, with peak currents from 5 to 315 kA. As seen in Table 2, most RORDs (30) were positive amplitude perturbations.

433

434

435

436

437

We also calculate the CMC for the discharges that occur at the time of three RORD events (see Table 3 and Figure 5c for the VLF signal). These events are also related to the same storm cell as the "early" events a, b and c. From Table 3 it is clear that the total CMC is smaller for the RORD events than for the "early" events; however, the CMC increased for at least 600 ms in all three cases.

438

4.4 MF radio wave attenuation

439

440

441

442

443

444

445

446

447

448

449

450

As shown by Farges et al. (2007), the electromagnetic fields generated by lightning may heat electrons of the lower ionosphere causing millisecond-duration reduction of the amplitudes of signals from MF radio stations. To explore the relationship between such perturbations and lightning with and without elves, we identified 7 MF transmitters from www.mwlist.org, where the signals to the receiver pass over the storm. The measurement concept is shown in Figure 9. The top panel shows the broadband spectrogram corresponding to the elve at 03:57:56.578 UTC, the middle panel shows the corresponding narrow-band signal amplitudes of four MF stations at 540 kHz, 576 kHz, 630 kHz, and 891 kHz, and the bottom panel shows the GCPs of the signals from the transmitters to the receiver. The attenuation is most pronounced at 540 kHz, smaller for the three other frequencies and absent in the remaining three links. From the map, we see that the four links impacted pass close to the center of the elve.

451

452

453

454

455

For the 59 events with lightning and elves, at least one link is impacted in 86% of the cases, in line with the observation of Farges et al. (2007) for flashes over 60 kA. For the MF attenuation related to the 175 CG high-current strokes that did not produce elves, we found that 53% of the events had at least one attenuated link. The numbers are given in Table 4.

456 The same technique used by Farges et al. (2007) was systematically employed here
 457 to calculate the temporal variation of the attenuation amplitude. The peak attenuation,
 458 onset time, rise time and duration of the events were estimated for the seven MF radio
 459 links. The averaged values of links with perturbations are shown in Table 4 for the 59
 460 events with elves and the 175 without. The mean peak attenuation is stronger than found
 461 by Farges et al. (2007), however they showed that the peak attenuation increases with
 462 the peak current. The found value is coherent to the ones calculated for CG strokes with
 463 peak current higher than 125 kA. The onset and rise time mean values are like those of
 464 Farges et al. (2007), whereas the duration is shorter, particularly for strong CGs strokes
 465 that are 5-8 ms in Farges et al. (2007). Our MF measurements confirm that the phe-
 466 nomenon discussed by Farges et al. (2007) is also present when storms are further from
 467 the receiver. Regarding cases with and without elves, no difference can be seen for the
 468 amplitude but the rise time and durations are significantly shorter for the latter. This
 469 could suggest that the MF perturbations in case of no elves observations are due to short
 470 or dim elves not able to trigger the camera. We have indeed cases in absence of elves with
 471 P(E²) which are of the same order of magnitude as with elves.

	MF blackout	Peak att (dB)	Onset time (ms)	Rise time (ms)	Duration (ms)
Elve	86%	-16.30	1.01	1.20	3.44
No Elve	53%	-15.68	1.06	1.00	2.89

Table 4. Mean values for MF perturbations for lightning with and without elves.

472 5 Discussion

473 The only types of radio wave perturbations that are observed simultaneously with
 474 elves are the LOREs and the MF blackouts. We first discuss how they are related to elves,
 475 then continue with “early” VLF events and RORD events.

476 5.1 Elves, LOREs and MF blackouts

477 Our observations support the understanding that elves are associated with LORES
 478 (Haldoupis et al., 2013), while the early VLF perturbations and RORD events are dis-
 479 tinct from LOREs and have other origins. However, the observations also raise questions
 480 regarding the relationship between elves and LOREs. First of all, why did 78% of the
 481 elves occur without LOREs? Second, why do the LOREs vary in amplitude from 0.25
 482 dB to >1 dB? In the following, we try to answer what determines the generation and
 483 amplitude of a LORE.

484 The five strongest LOREs (at 20:09, 22:48, 01:33, 02:19, and 3:56 UTC) have am-
 485 plitude decreases close to, or larger than, 1 dB. We refer to them as sLOREs (strong)
 486 and the rest as wLORE (weak). As seen from Table 1, the presence or amplitude of LOREs
 487 is not mirrored in the parameters derived from the ELF data. For instance, the current
 488 moment was smaller for cases with weak or absent LOREs, but not significantly so. We
 489 cannot, then, search for an explanation in the ELF data. Turning to the VLF data, Marshall
 490 and Inan (2010) present a finite difference, frequency domain model of narrow-band VLF
 491 transmitter signal propagation in the Earth-ionosphere wave-guide. They place an elec-
 492 tron density perturbation at the ionospheric boundary at 85 km somewhere along the
 493 propagation path and calculate the changes in the signal properties at a receiver. They
 494 show that the amplitude perturbation can be both positive and negative, that it is most

495 perturbed if the disturbance is where the amplitude at the ground is low, such as an in-
 496 terference null, and can be suppressed entirely if it falls at an interference null at the re-
 497 flection altitude. The amplitude also depends on parameters such as the path length,
 498 ionospheric and ground properties, and the signal frequency, however, the night-time elec-
 499 tron density fluctuations have a minor influence. In line with their model, we find both
 500 positive and negative perturbations in the amplitude and no dependence in local time
 501 of the occurrence of LOREs and their amplitudes.

502 In Figure 7a, we show the location given by GLD360 of the CG strokes that pro-
 503 duced elves and LOREs (also "early" and RORD events), and panel c is a zoom of a re-
 504 gion close to the VLF path. As noted earlier, Figure 7a shows that the location of all
 505 negative LOREs is similar but remarkably different for the positive LOREs. However,
 506 the strong LOREs (light blue squares in Figure 7c) are not found closer or at a differ-
 507 ent geometry relative to the VLF path than the weak LOREs (dark blue diamonds in
 508 Figure 7c). Likewise, although many of the elves without LOREs are at a greater dis-
 509 tance and different location relative to the VLF signal path, such as those of the cell at
 510 $\sim 42.8^\circ\text{N}$, $\sim 14.5^\circ\text{E}$, some are very close (see Figure 7c). The observations confirm the
 511 model results of Marshall and Inan (2010) and observations in Naitamor et al. (2013)
 512 that the relative location of the lightning/disturbance and the VLF path is important
 513 for the amplitude and sign of LOREs. It may not be the whole story, though, because
 514 we also see from Figure 10a that elves with LOREs are brighter and produced by strokes
 515 of higher power, $P(E^2)$, and that the strong LOREs are among the highest in this group.
 516 This observation implies that the stroke energy should be large enough to create appre-
 517 ciable ionization before we can observe a LORE. From Figure 10b, we see that the al-
 518 titude could also be relevant since all elves associated with LOREs were above 86 km.
 519 The altitude limit suggested by our results could be related to the reflection height of
 520 the VLF signal, which according to Ratcliffe (1959, Figure 12.1) is ~ 86 km for this par-
 521 ticular frequency of 45.9 kHz.

522 We next turn to the MF blackouts. Since both LOREs and MF blackouts are re-
 523 lated to elves, although linked to different processes in the elve generation (ionization
 524 and heating, respectively), we looked in our data for a relationship between the two types
 525 of phenomena. Figure 10a, b, show that the elves without MF blackouts were caused by
 526 lightning with power from 22-56 $(\text{V/m})^2$. However, many elves in this range were also
 527 found with MF blackouts. Thus, we cannot determine a threshold. The data in Figure
 528 10b could suggest that elves at lower altitudes are more likely to be related to MF black-
 529 outs, however, such a conclusion would be uncertain. It is also uncertain if the location
 530 of the disturbance relative to the signal path plays a role. In the region shown in Fig-
 531 ure 7c, all but one elve created MF blackouts, which is the same proportion as overall.
 532 Understanding the relationship between elves, LOREs and MF blackouts appear to re-
 533 quire extensive modeling in addition to data analysis. We can, however, state that MF
 534 blackouts may occur without LOREs, but not LOREs without MF blackouts. Accord-
 535 ing to current theories for the two types of perturbations, this statement corresponds to
 536 the presence of heating without ionization but not ionization without heating.

537 5.2 "Early" and RORD events

538 We can now discuss the origin of the other types of perturbation. The physical mech-
 539 anisms responsible for early VLF events are still under debate. The candidate mecha-
 540 nisms that have gained the most attention are that they are a result of scattering from
 541 ionization regions associated with sprites and/or halos (Haldoupis et al., 2004; Moore
 542 et al., 2003). Although the camera horizon was below 70 km for 74% of the "early" events,
 543 we do not see optical signatures of sprites or halos. Therefore, we suggest that the "early"
 544 VLF events were caused by density changes in the mesosphere that did not produce op-
 545 tical emission.

546 Marshall et al. (2008) showed that density changes in the lower ionosphere by elec-
 547 tron losses through dissociative attachment to molecular oxygen can create measurable
 548 amplitude changes in VLF transmitter signals that travel through the disturbed region.
 549 The energy required for attachment (3.7 eV) is lower than that of N₂ optical emissions
 550 often seen in sprites and elves (7.5 eV) and N₂ and O₂ ionization (15.6 eV) (Haldoupis
 551 et al., 2006; Neubert & Chanrion, 2013). This implies that attachment can occur with-
 552 out optical emission and ionization, explaining why we and other studies (e.g., Marshall
 553 et al., 2006) report "early" events without associated optical emissions, and also why op-
 554 tical emissions without "early" events are rare (Haldoupis et al., 2004, 2010). The timescale
 555 of attachment at ~70 km altitude with high electric fields, but below the threshold field
 556 for discharges, is around 0.1 ms while the timescales for screening out the field (the di-
 557 electric relaxation time τ_{σ}) is around 10 ms (Neubert & Chanrion, 2013). This means
 558 that electric fields may last long enough for attachment to change the density and thereby
 559 the conductivity of the bottom ionosphere introducing perturbations in VLF signals. The
 560 timescales of recovery for density changes in the lower ionosphere controlled by attachment-
 561 detachment processes is in the order of 100 s (Pasko & Inan, 1994), consistent with the
 562 recovery times of the "early" events. As discussed in (Marshall et al., 2008), a consequence
 563 of this hypothesis is that "early" VLF events caused by attachment-depleted regions would
 564 mostly have positive perturbation amplitudes due to less VLF signal absorption in the
 565 reduced density region. This scenario is consistent with our results as well as results from
 566 other previous studies (e.g., Inan et al., 1993; Inan, Sampson, & Taranenko, 1996; Mar-
 567 shall et al., 2006; Haldoupis et al., 2004).

568 Marshall et al. (2008) attribute the attachment process to the EMP from succes-
 569 sive in-cloud lightning discharges. Because we observe very high CMC related to the early
 570 events (Table 3), we suggest that the QE field caused by the CMC related to the dis-
 571 charges could also contribute to attachment, either alone or in combination with the EMP.
 572 The CMC appears high enough to produce ionization in the mesosphere. Common thresh-
 573 old values for breakdown in the lower ionosphere are about 600 C km (Cummer & Lyons,
 574 2005), and for winter thunderstorms, sprite producing strokes were found to have aver-
 575 age CMC values of 1400 ± 600 C km, with only extreme events exceeding 3500 C km
 576 (Yair et al., 2009). However, we know from Pasko et al. (1997) and it is demonstrated
 577 and generalized in Hiraki and Fukunishi (2006), that the electric field in the mesosphere
 578 depends on the CMC but also on the the timescale of charge removal. Sprites and ha-
 579 los usually occur after an impulsive enhancement of the CMC by lightning flash or cur-
 580 rent in the continuing discharge in the order of milliseconds. From Figure 8, we see that
 581 the events are related to long (~ 500 ms) sequences of discharges, with both larger and
 582 smaller discharges some of which are slower than typically and probably related to IC
 583 activity. The CMC increases during 10-100 ms, which is likely too slow to produce TLEs.
 584 It could, however, be sufficient to increase attachment (Neubert & Chanrion, 2013) that
 585 would lower the electron density and perturb the VLF transmitter signal that passes through
 586 the affected region.

587 The short-duration RORD events in which the entire signal amplitude change lasts
 588 only for 0.5-2 seconds are consistent with the heating of the ambient electrons by QE
 589 fields in cases when heating is not intense enough to exceed the attachment (3.7 eV) or
 590 ionization thresholds (15.6 eV). According to this hypothesis, RORD events are equiv-
 591 alent to the MF blackouts. The conductivity changes due to heating alone last only as
 592 long as the fields, which is typically a few seconds for QE fields (Inan, Slingeland, et al.,
 593 1996) and only ms for the EMP (Farges et al., 2007). When heating energy exceeds at-
 594 tachment or ionization thresholds, the electron density is reduced or enhanced respec-
 595 tively, in which case the medium would relax back to the ambient conditions in the time
 596 scales of the local chemistry (typically 10-100 seconds at sprite altitudes (Pasko & Inan,
 597 1994; Rodger et al., 1998)), as is the case in "early" events. The CMCs associated to the
 598 four RORD events in Table 3 are clearly smaller than for the early events while their time
 599 constants are the same, supporting this theory.

600 6 Summary

601 We analyze for the first time observations of a large number of elves (63) from a
 602 single storm over the Adriatic Sea and associated perturbations to MF and VLF trans-
 603 mitter signals. We find three types of perturbations in the VLF transmitter signal: LOREs,
 604 "early" and RORD events. We also analyze the iCMC and CMC of selected lightning
 605 strokes. Based on the observations, we conclude that:

- 606 1. Elves are either accompanied by LOREs (14) or no perturbation (49). Thus, elves
 607 are not observed with other types of perturbations in the VLF transmitter signal.
- 608 2. Our results suggest that bright elves at higher altitudes (>86 km) generated by
 609 high energy strokes are primarily associated with LOREs.
- 610 3. The sign of the LORE amplitude perturbation depends on the location of the dis-
 611 turbance (elve) relative to the VLF TR path.
- 612 4. MF blackouts occur more often with elves (86 %) than with CG strokes of sim-
 613 ilar high current, but without elves (53 %).
- 614 5. CG strokes that produce elves have one order of magnitude higher power $P(E^2)$
 615 and three times higher iCMC than strokes of similar peak current that do not pro-
 616 duce elves.
- 617 6. "Early" and RORD events correlate with lightning sequences with slowly increas-
 618 ing CMCs (400 ms) that reach high values. The CMC is higher for early events
 619 (>3535 C km) than for RORD events (>1176 C km).
- 620 7. Both early and RORD events are, in some cases, observed exclusively with IC dis-
 621 charges.

622 Acknowledgments

623 This study was made with the use of NSY transmitter data provided by R. Slošiar from
 624 the SOSA (Slovak Organization for Space Activities), Bratislava, Slovakia, and for this
 625 we are grateful. The authors thank Laboratoire Souterrain à Bas Bruit (LSBB), Rus-
 626 trel, France, and its staff, for hosting our camera system. We also thank Vaisala and Ryan
 627 Said for providing GLD360 lightning data. And Jeff Lapierre and Earth Networks for light-
 628 ning activity data and useful discussions. In addition we thank Martin Füllerkrug for
 629 interesting discussions on lightning waveforms. The authors thank the French AERIS/ICARE
 630 Data and Services Center which provided MSG/SEVIRI data for cloud top temperature.
 631 They thank the European Copernicus/ECMWF Data Center, for providing ERA5 me-
 632 teorological reanalysis. The work of IK was supported by the GACR grant 20-0967S. J.
 633 Mlynarczyk acknowledges support of the National Science Centre, Poland, under grant
 634 2015/19/B/ ST10/01055.

635 Data availability

636 The data used for this publication can be obtained from the public repository (xxx)
 637 will be available by acceptance xxx).

638 References

- 639 Barrington-Leigh, C. P., & Inan, U. S. (1999). Elves triggered by positive and neg-
 640 ative lightning discharges. *Geophysical Research Letters*, *26*(6), 683–686. doi:
 641 10.1029/1999GL900059
- 642 Blaes, P. R., Marshall, R. A., & Inan, U. S. (2016). Global occurrence rate of elves
 643 and ionospheric heating due to cloud-to-ground lightning. *Journal of Geophys-*
 644 *ical Research A: Space Physics*, *121*(1), 699–712. doi: 10.1002/2015JA021916
- 645 Boeck, W. L., Vaughan, O. H., Blakeslee, R., Vonnegut, B., & Brook, M. (1992).
 646 Lightning induced brightening in the airglow layer. *Geophysical Research*

- 647 *Letters*, 19(2), 99–102. doi: 10.1029/91GL03168
- 648 Burgess, W. C. (1993). The Role of Ducted Whistlers in the Precipitation Loss and
649 Equilibrium Flux. , 98.
- 650 Chen, A. B., Kuo, C.-L., Lee, Y.-J., Su, H.-T., Hsu, R.-R., Chern, J.-L., . . . Lee,
651 L.-C. (2008). Global distributions and occurrence rates of transient lumi-
652 nous events. *Journal of Geophysical Research: Space Physics*, 113(A8). doi:
653 10.1029/2008JA013101
- 654 Chen, A. B., Su, H.-T., & Hsu, R.-R. (2014). Energetics and geographic distribu-
655 tion of elve-producing discharges. *JGR Space physics*, 119, 1–24. doi: 10.1002/
656 2013JA019470
- 657 Cummer, S. A., & Lyons, W. A. (2004). Lightning charge moment changes in U.S.
658 High Plains thunderstorms. *Geophysical Research Letters*, 31(5). doi: 10.1029/
659 2003GL019043
- 660 Cummer, S. A., & Lyons, W. A. (2005). Implications of lightning charge moment
661 changes for sprite initiation. *Journal of Geophysical Research: Space Physics*,
662 110(A4), 1–9. doi: 10.1029/2004JA010812
- 663 Dowden, R. L., Adams, C. D., Brundell, J. B., & Dowden, P. E. (1994). Rapid on-
664 set, rapid decay (RORD), phase and amplitude perturbations of VLF subiono-
665 spheric transmissions. *Journal of Atmospheric and Terrestrial Physics*, 56(11),
666 1513–1527. doi: 10.1016/0021-9169(94)90118-X
- 667 Farges, T., & Blanc, E. (2011). Champs électriques induits par les éclairs et les
668 événements lumineux transitoires et leur effet sur l’ionosphère. *Comptes Ren-
669 dus Physique*, 12(2), 171–179. doi: 10.1016/j.crhy.2011.01.013
- 670 Farges, T., Blanc, E., & Tanguy, M. (2007). Experimental evidence of D region heat-
671 ing by lightning-induced electromagnetic pulses on MF radio links. *J. Geophys.
672 Res*, 112, 10302. doi: 10.1029/2007JA012285
- 673 Fukunishi, H., Takahashi, Y., & Sakanoi, K. (1996). Elves: Lightning-induced tran-
674 sient luminous events in the lower ionosphere. , 23(16), 2157–2160.
- 675 Haldoupis, C., Amvrosiadi, N., Cotts, B. R. T., van der Velde, O. A., Chanrion, O.,
676 & Neubert, T. (2010). More evidence for a one-to-one correlation between
677 Sprites and Early VLF perturbations . *Journal of Geophysical Research: Space
678 Physics*, 115(A7), 1–11. doi: 10.1029/2009ja015165
- 679 Haldoupis, C., Cohen, M., Arnone, E., Cotts, B., & Dietrich, S. (2013). The VLF
680 fingerprint of elves: Step-like and long-recovery early VLF perturbations
681 caused by powerful \pm cG lightning em pulses. *Journal of Geophysical Research:
682 Space Physics*, 118(8), 5392–5402. doi: 10.1002/jgra.50489
- 683 Haldoupis, C., Neubert, T., Inan, U. S., Mika, A., Allin, T. H., & Marshall, R. A.
684 (2004). Subionospheric early VLF signal perturbations observed in one-to-one
685 association with sprites. *Journal of Geophysical Research: Space Physics*,
686 109(A10), 10303. doi: 10.1029/2004JA010651
- 687 Haldoupis, C., Steiner, R. J., Mika, , Shalimov, S., Marshall, R. A., Inan, U. S., . . .
688 Neubert, T. (2006). “Early/slow” events: A new category of VLF perturba-
689 tions observed in relation with sprites. *Journal of Geophysical Research: Space
690 Physics*, 111(A11). doi: 10.1029/2006JA011960
- 691 Hiraki, Y., & Fukunishi, H. (2006). Theoretical criterion of charge moment change
692 by lightning for initiation of sprites. *Journal of Geophysical Research: Space
693 Physics*, 111(11), 1–6. doi: 10.1029/2006JA011729
- 694 Inan, U. S., Bell, T. F., Pasko, V. P., Sentman, D. D., Wescott, E. M., & Lyons,
695 W. A. (1995). VLF signatures of ionospheric disturbances associated
696 with sprites. *Geophysical Research Letters*, 22(24), 3461–3464. doi:
697 10.1029/95GL03507
- 698 Inan, U. S., Rodriguez, J. V., & Idone, V. P. (1993). VLF signatures of lightning-
699 induced heating and ionization of the nighttime D-region. *Geophysical Re-
700 search Letters*, 20(21), 2355–2358. doi: 10.1029/93GL02620
- 701 Inan, U. S., Sampson, W. A., & Taranenko, Y. N. (1996). Space-time structure of

- 702 optical flashes and ionization changes produced by lightning-EMP. *Geophysical*
703 *Research Letters*, *23*(2), 133–136. doi: 10.1029/95GL03816
- 704 Inan, U. S., Slingeland, A., Pasko, V. P., & Rodriguez, J. V. (1996). VLF and LF
705 signatures of mesospheric/lower ionospheric response to lightning discharges.
706 *Journal of Geophysical Research: Space Physics*, *101*(A3), 5219–5238. doi:
707 10.1029/95ja03514
- 708 Johnson, M. P., & Inan, U. S. (2000). Sferic Clusters Associated with Early / Fast
709 VLF Events Early / Fast Event Association with. *Geophysical Research Let-*
710 *ters*, *27*(9), 1391–1394.
- 711 Kabirzadeh, R., Marshall, R. A., & Inan, U. S. (2017). Early/fast VLF events
712 produced by the quiescent heating of the lower ionosphere by thunderstorms.
713 *Journal of Geophysical Research: Atmospheres*, *122*(12), 6217–6230. doi:
714 10.1002/2017JD026528
- 715 Kolmašová, I., Santolík, O., Kašpar, P., Popek, M., Pizzuti, A., Spurný, P., ...
716 Slošiar, R. (2021). First Observations of Elves and Their Causative Very
717 Strong Lightning Discharges in an Unusual Small-Scale Continental Spring-
718 Time Thunderstorm. *Journal of Geophysical Research: Atmospheres*, *126*(1),
719 1–23. doi: 10.1029/2020JD032825
- 720 Lu, G., Cummer, S. A., Blakeslee, R. J., Weiss, S., & Beasley, W. H. (2012). Light-
721 ning morphology and impulse charge moment change of high peak current
722 negative strokes. *Journal of Geophysical Research Atmospheres*, *117*(4), 1–16.
723 doi: 10.1029/2011JD016890
- 724 Mallick, S., Rakov, V. A., Hill, J. D., Ngin, T., Gamerota, W. R., Pilkey, J. T., ...
725 Nag, A. (2014). Performance characteristics of the NLDN for return strokes
726 and pulses superimposed on steady currents, based on rocket-triggered light-
727 ning data acquired. *Journal of Geophysical Research: Atmospheres*, *119*,
728 3825–3856. doi: 10.1002/2013JD021401
- 729 Marshall, R. A. (2012). An improved model of the lightning electromagnetic field
730 interaction with the D-region ionosphere. *Journal of Geophysical Research:*
731 *Space Physics*, *117*(3), 1–15. doi: 10.1029/2011JA017408
- 732 Marshall, R. A., & Inan, U. S. (2010). Two-dimensional frequency domain
733 modeling of lightning EMP-induced perturbations to VLF transmitter sig-
734 nals. *Journal of Geophysical Research: Space Physics*, *115*(A6), 0–29. doi:
735 10.1029/2009JA014761
- 736 Marshall, R. A., Inan, U. S., & Chevalier, T. W. (2008, 11). Early VLF perturba-
737 tions caused by lightning EMP-driven dissociative attachment. *Geophysical Re-*
738 *search Letters*, *35*(21). doi: 10.1029/2008GL035358
- 739 Marshall, R. A., Inan, U. S., & Glukhov, V. S. (2010). Elves and associated electron
740 density changes due to cloud-to-ground and in-cloud lightning discharges. *J.*
741 *Geophys. Res.*, *115*, 0–17. doi: 10.1029/2009JA014469
- 742 Marshall, R. A., Inan, U. S., & Lyons, W. A. (2006). On the association of
743 early/fast very low frequency perturbations with sprites and rare examples
744 of VLF backscatter. *Journal of Geophysical Research: Atmospheres*, *111*,
745 19108. doi: 10.1029/2006JD007219
- 746 Mika, A., Haldoupis, C., Neubert, T., Su, H. T., Hsu, R. R., Steiner, R. J., &
747 Marshall, R. A. (2006). Early VLF perturbations observed in associa-
748 tion with elves. *Annales Geophysicae*, *24*(8), 2179–2189. doi: 10.5194/
749 angeo-24-2179-2006
- 750 Mlynarczyk, J., Bór, J., Kulak, A., Popek, M., & Kubisz, J. (2015). An unusual
751 sequence of sprites followed by a secondary TLE: An analysis of ELF radio
752 measurements and optical observations. *Journal of Geophysical Research:*
753 *Space Physics*, *120*, 2241–2254. doi: 10.1002/2014JA020780
- 754 Moore, R. C., Barrington-Leigh, C. P., Inan, U. S., & Bell, T. F. (2003, 10).
755 Early/fast VLF events produced by electron density changes associated with
756 sprite halos. *Journal of Geophysical Research: Space Physics*, *108*. doi:

- 10.1029/2002JA009816
- 757 Naitamor, S., Cohen, M. B., Cotts, B. R., Ghalila, H., Alabdoadaim, M. A., & Graf,
758 K. (2013). Characteristics of long recovery early VLF events observed by the
759 North African AWESOME Network. *Journal of Geophysical Research: Space*
760 *Physics*, *118*(8), 5215–5222. doi: 10.1002/jgra.50448
- 761 Neubert, T., & Chanrion, O. (2013). On the electric breakdown field of the meso-
762 sphere and the influence of electron detachment. *Geophysical Research Letters*,
763 *40*(10), 2373–2377. doi: 10.1002/grl.50433
- 764 Pasko, V. P., & Inan, U. S. (1994). Recovery signatures of lightning-associated VLF
765 perturbations as a measure of the lower ionosphere. *JGR Space physics*. doi:
766 <https://doi.org/10.1029/94JA01378>
- 767 Pasko, V. P., Inan, U. S., Bell, T. F., & Taranenko, Y. N. (1997). Sprites pro-
768 duced by quasi-electrostatic heating and ionization in the lower ionosphere.
769 *Journal of Geophysical Research: Space Physics*, *102*(A3), 4529–4561. doi:
770 10.1029/96JA03528
- 771 Peter, W. B., & Inan, U. S. (2007). A quantitative comparison of lightning-induced
772 electron precipitation and VLF signal perturbations. *Journal of Geophysical*
773 *Research: Space Physics*, *112*(12), 1–20. doi: 10.1029/2006JA012165
- 774 Ripoll, J.-F., Farges, T., Malaspina, D. M., Cunningham, G. S., Lay, E. H.,
775 Hospodarsky, G. B., . . . Pédeboy, . S. (2021). Electromagnetic power of
776 lightning superbolts from Earth to space. *Nature communications*. doi:
777 10.1038/s41467-021-23740-6
- 778 Rodger, C. J. (2003). Subionospheric VLF perturbations associated with lightning
779 discharges. *Journal of Atmospheric and Solar-Terrestrial Physics*, *65*(5), 591–
780 606. doi: 10.1016/S1364-6826(02)00325-5
- 781 Rodger, C. J., Molchanov, O. A., & Thomson, N. R. (1998, 4). Relaxation of tran-
782 sient ionization in the lower ionosphere. *Journal of Geophysical Research:*
783 *Space Physics*, *103*(A4), 6969–6975. doi: 10.1029/98JA00016
- 784 Said, R. K., Inan, U. S., & Cummins, K. L. (2010). Long-range lightning geolo-
785 cation using a VLF radio atmospheric waveform bank. *Journal of Geophysical*
786 *Research Atmospheres*, *115*(23), 1–19. doi: 10.1029/2010JD013863
- 787 Said, R. K., & Murphy, M. J. (2016). GLD360 Upgrade: Performance Analysis and
788 Applications. In *24th international lightning detection conference*.
- 789 Salut, M. M., Abdullah, M., Graf, K. L., Cohen, M. B., Cotts, B. R., & Kumar,
790 S. (2012). Long recovery VLF perturbations associated with lightning dis-
791 charges. *Journal of Geophysical Research: Space Physics*, *117*(8), 1–6. doi:
792 10.1029/2012JA017567
- 793 van der Velde, O. A., & Montanyà, J. (2016). Statistics and variability of the alti-
794 tude of elves. *Geophysical Research Letters*, *43*(10), 5467–5474. doi: 10.1002/
795 2016GL068719
- 796 Yair, Y., Price, C., Ganot, M., Greenberg, E., Yaniv, R., Ziv, B., . . . Satori, G.
797 (2009). Optical observations of transient luminous events associated with win-
798 ter thunderstorms near the coast of Israel. *Atmospheric Research*, *91*(2-4),
799 529–537. doi: 10.1016/j.atmosres.2008.06.018
- 800

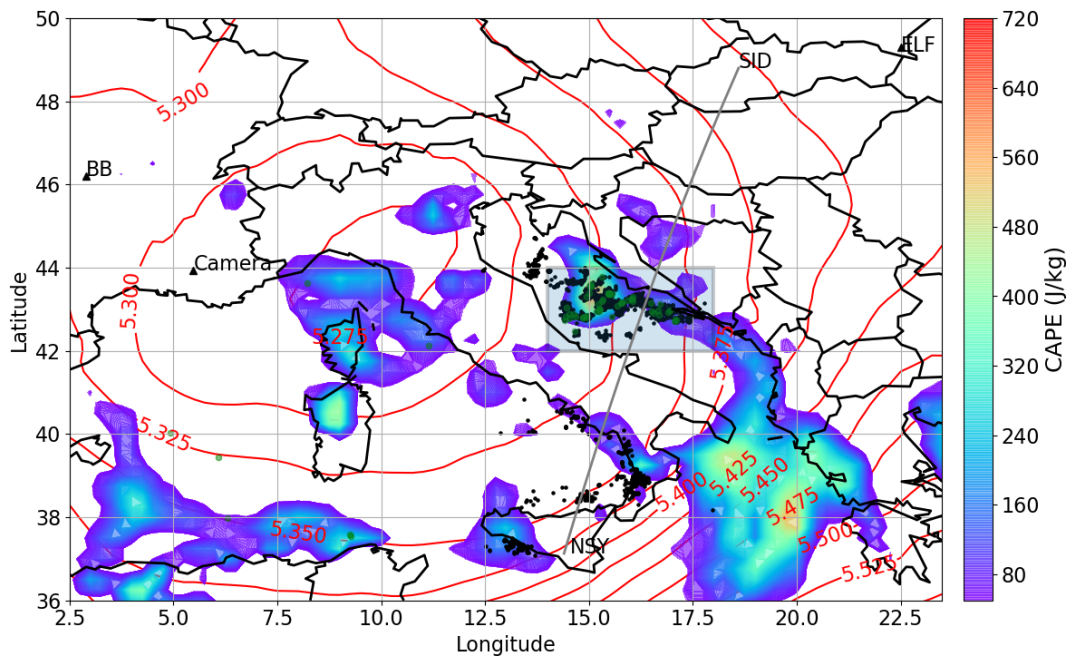


Figure 1. Overview map showing the location of instrumentation used in this study. All CG lightning strokes within ~ 250 km from the GCP of the VLF signal are plotted in black and the elve producing strokes in green. Red contour lines show the geopotential height at 500 hPa and CAPE is shown in colors. The rectangle frames the region where the elves were observed.

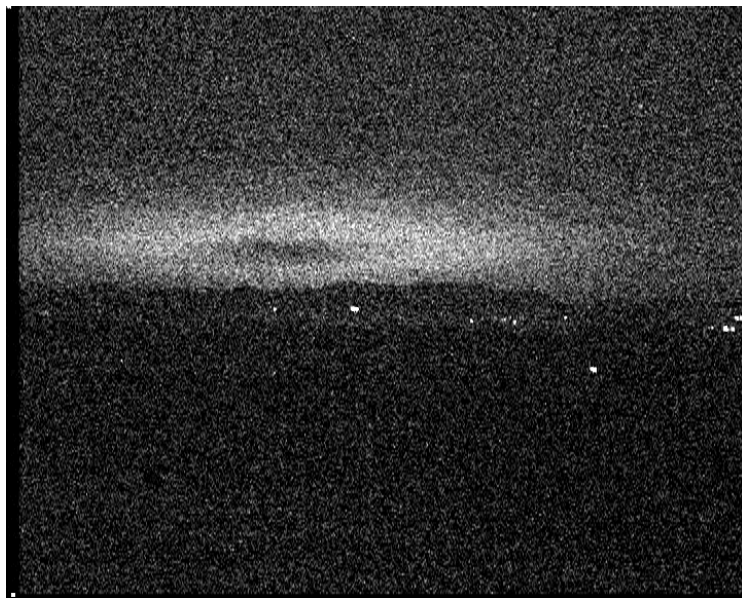


Figure 2. Example of elve image from this study. This elve appeared on December 10 2020, at 03:57:56.578 UTC.

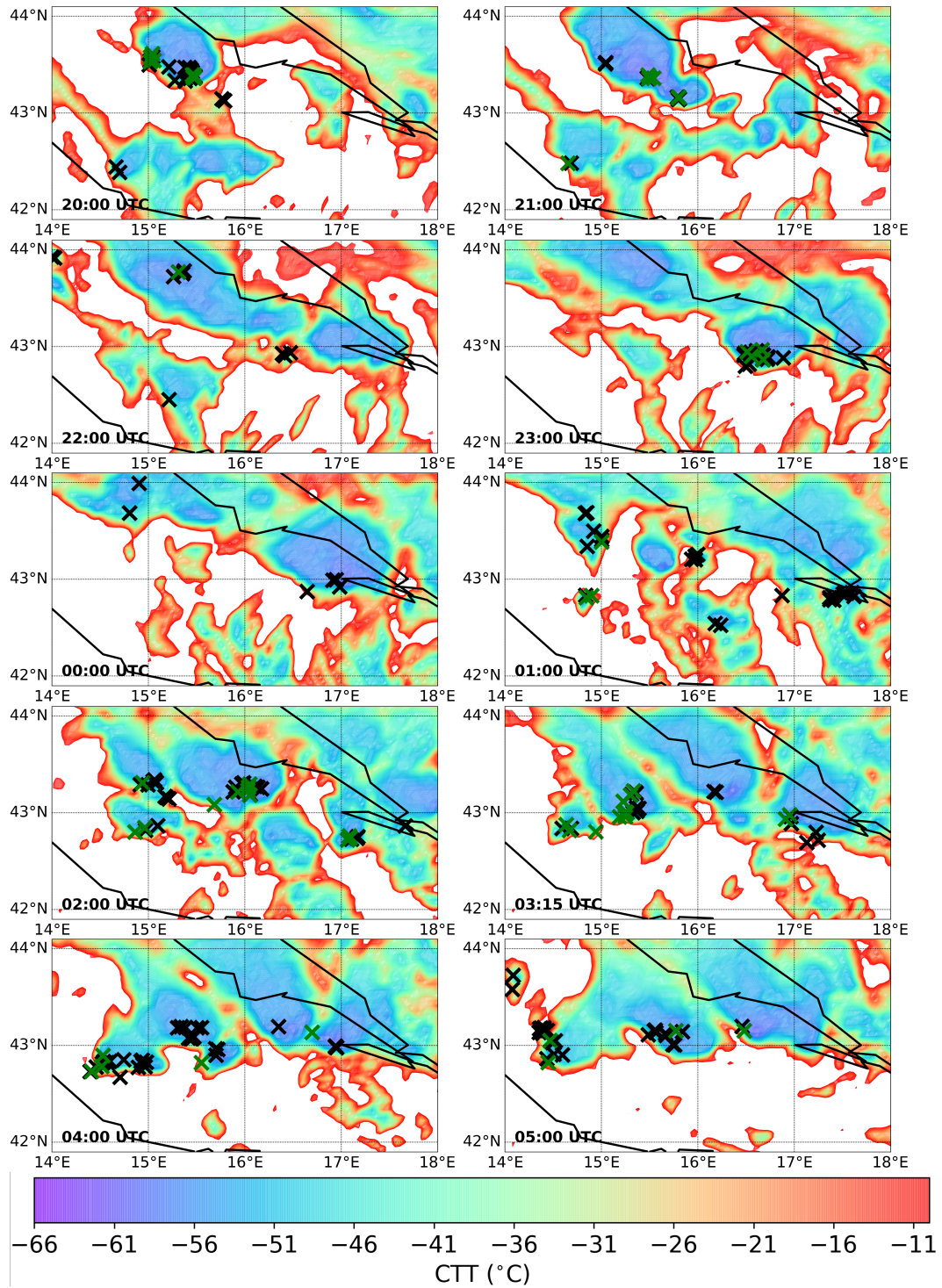


Figure 3. Hourly snapshots of cloud top temperature and strokes with peak currents absolute values higher than 200 kA marked with black crosses from 20 to 05 UTC. The elve-producing strokes are plotted in green.

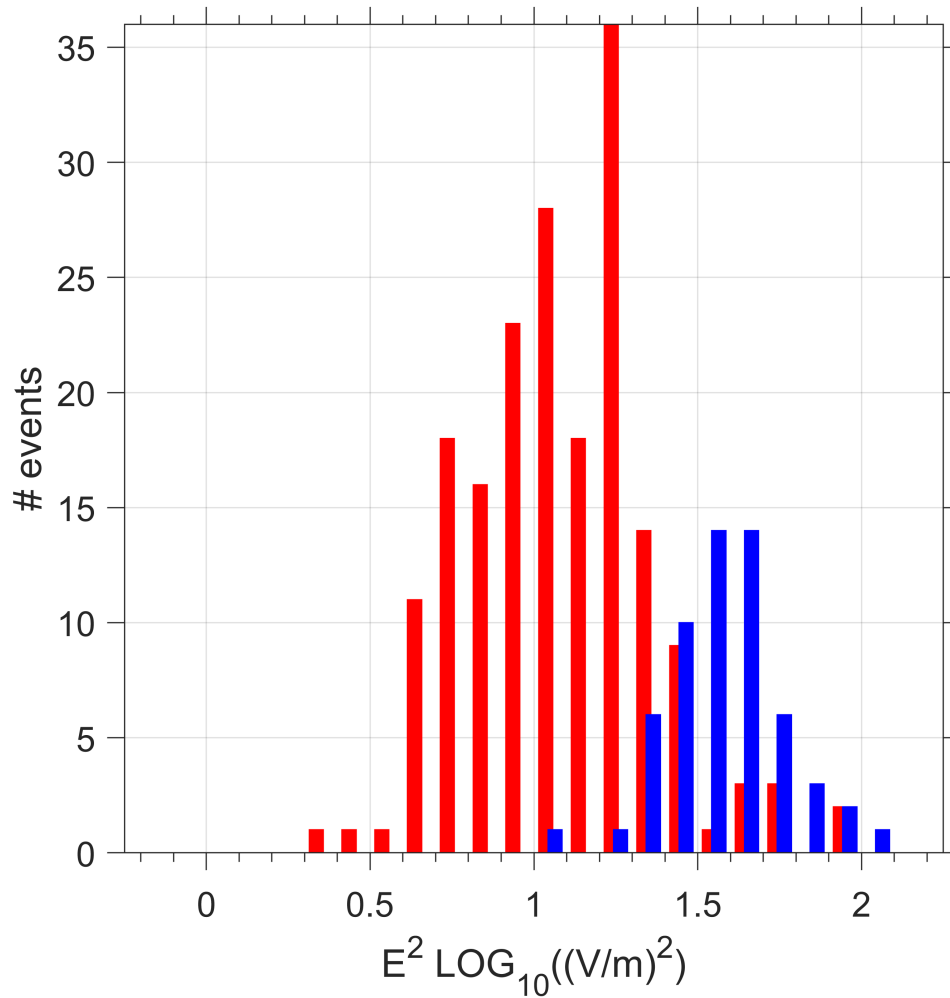


Figure 4. The $P(E^2)$ of the electric field in the band from 1 kHz to 5 MHz computed over 1.5 ms.

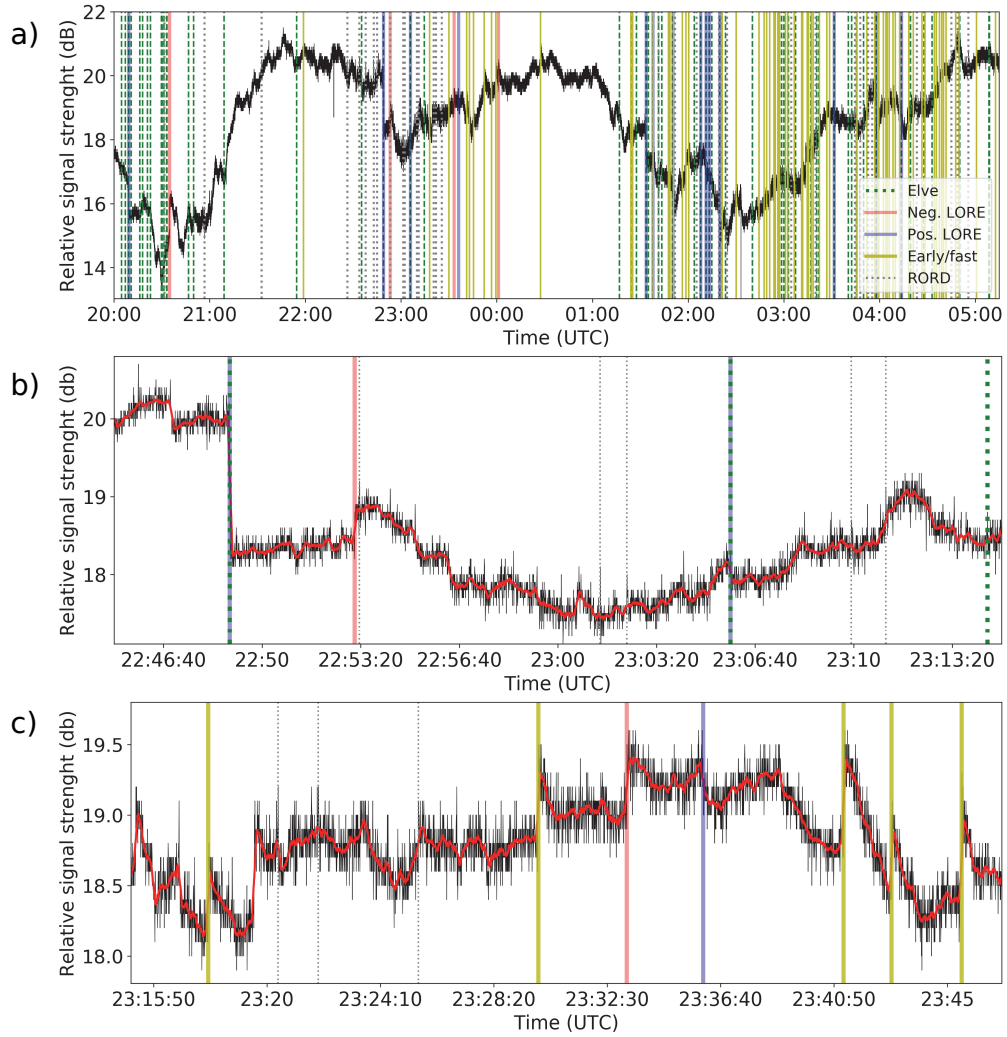


Figure 5. (a) Intensity of the NSY VLF signal (45.9 kHz) recorded in Bojnice (Slovakia) on the night of December 9-10, 2020. Overlaid are the times of elves, LOREs, "early" events and RORD events. b) A zoom of the signal in the time 22:45-23:15 UTC. c) A zoom of the signal in the time 23:15-23:47 UTC.

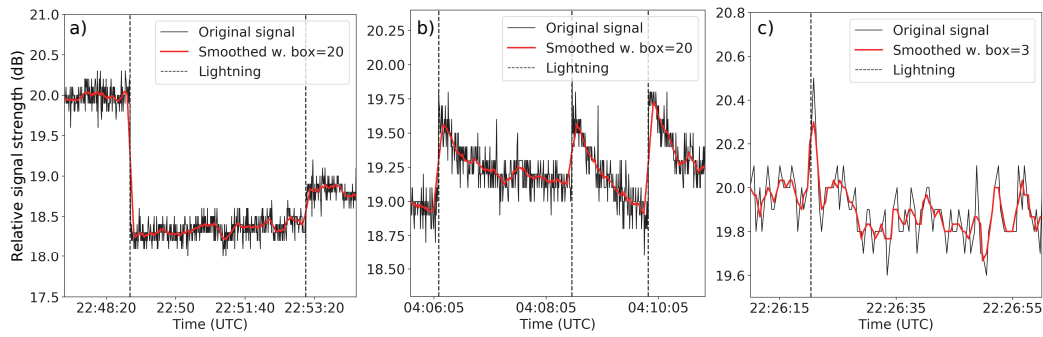


Figure 6. a) An example of a negative and positive LOR event. The negative LOR is caused by a lightning stroke of -725 kA that also produced an elve. The positive LOR is caused by a -530 kA stroke which would likely produce an elve, but the camera was not pointed towards its direction. b) Three examples of "early" events. The first and third have simultaneous strokes with -121 kA and $+59$ kA currents. The second has no identified stroke but coincides with an IC pulse of -7 kA. c) An example of a RORD event caused by a -155 kA stroke.

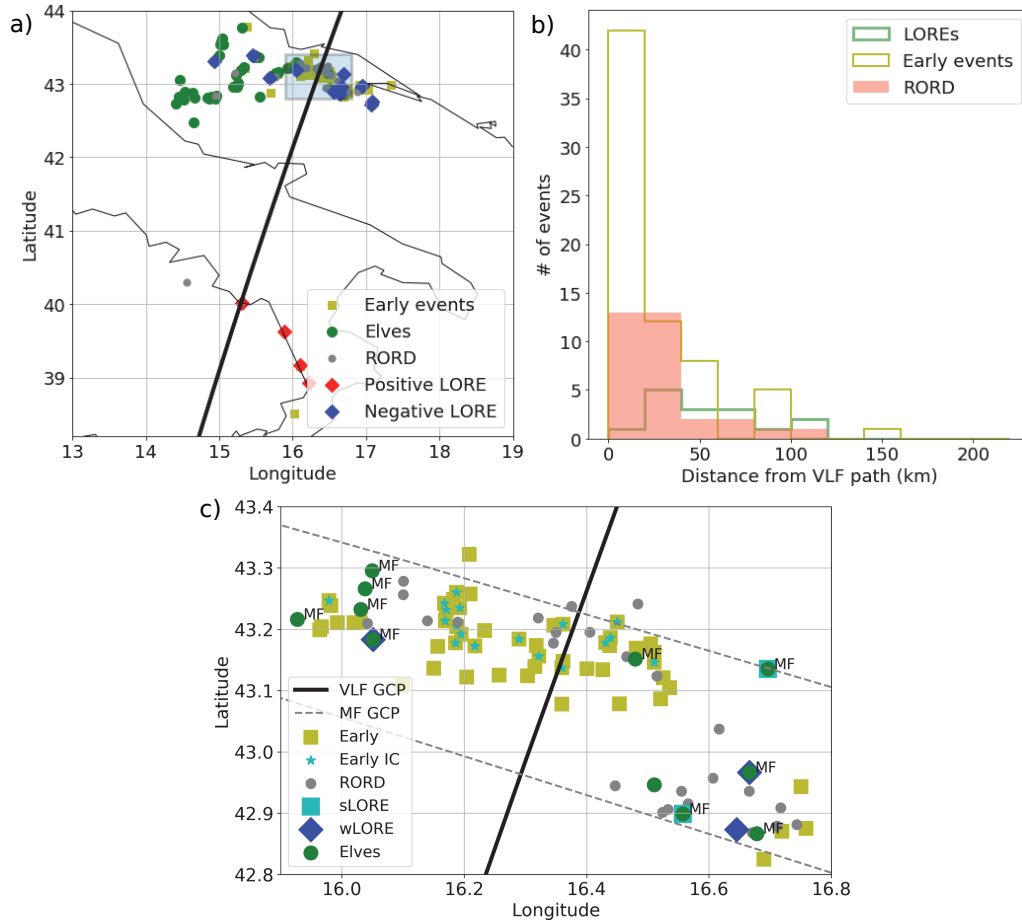


Figure 7. a) Locations of elve-producing strokes (green dots) and LOR-producing strokes (blue/red diamonds). The CG strokes responsible for "early" events are shown with yellow squares and RORD with gray circles. The VLF GCP is shown in black. b) Histogram showing the distance between causative lightning stroke and VLF GCP for the three types of events. c) Zoom to the region marked with a rectangle in panel a). In addition to the markers in panel a), we highlight the strong LORs (>1 dB) with cyan marker, the "early" events produced by IC pulses with cyan stars and annotate MF blackouts related to an elve. Gray dashed lines are MF GCPs that cross this region.

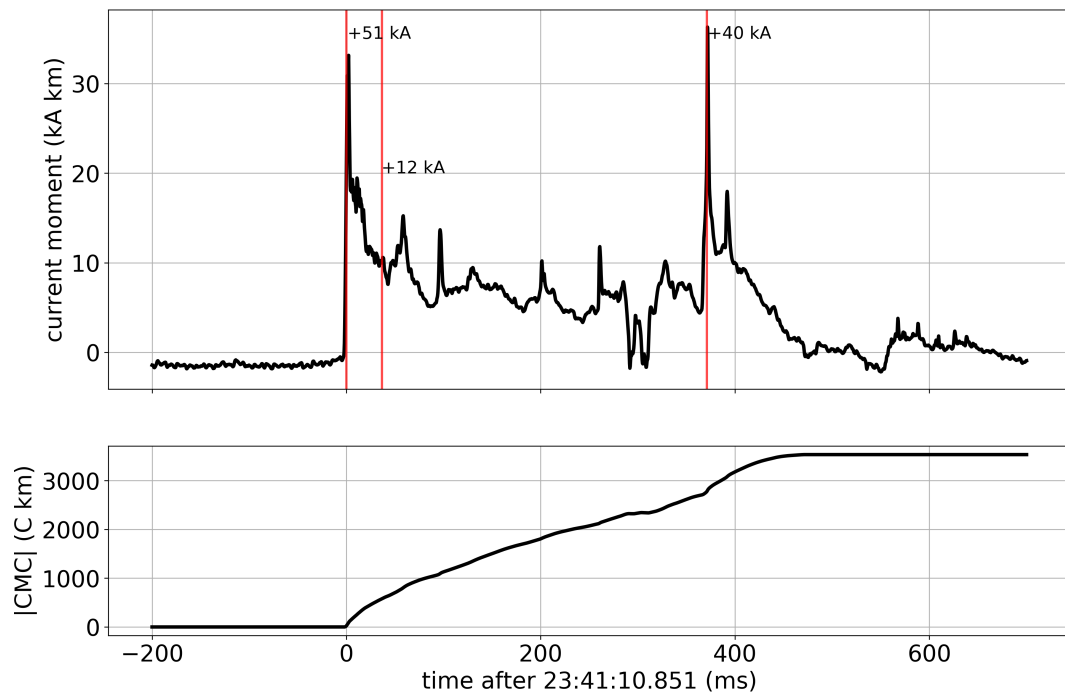


Figure 8. Current moment and charge moment change for "early" event c. The three CG strokes are detected by GLD360.

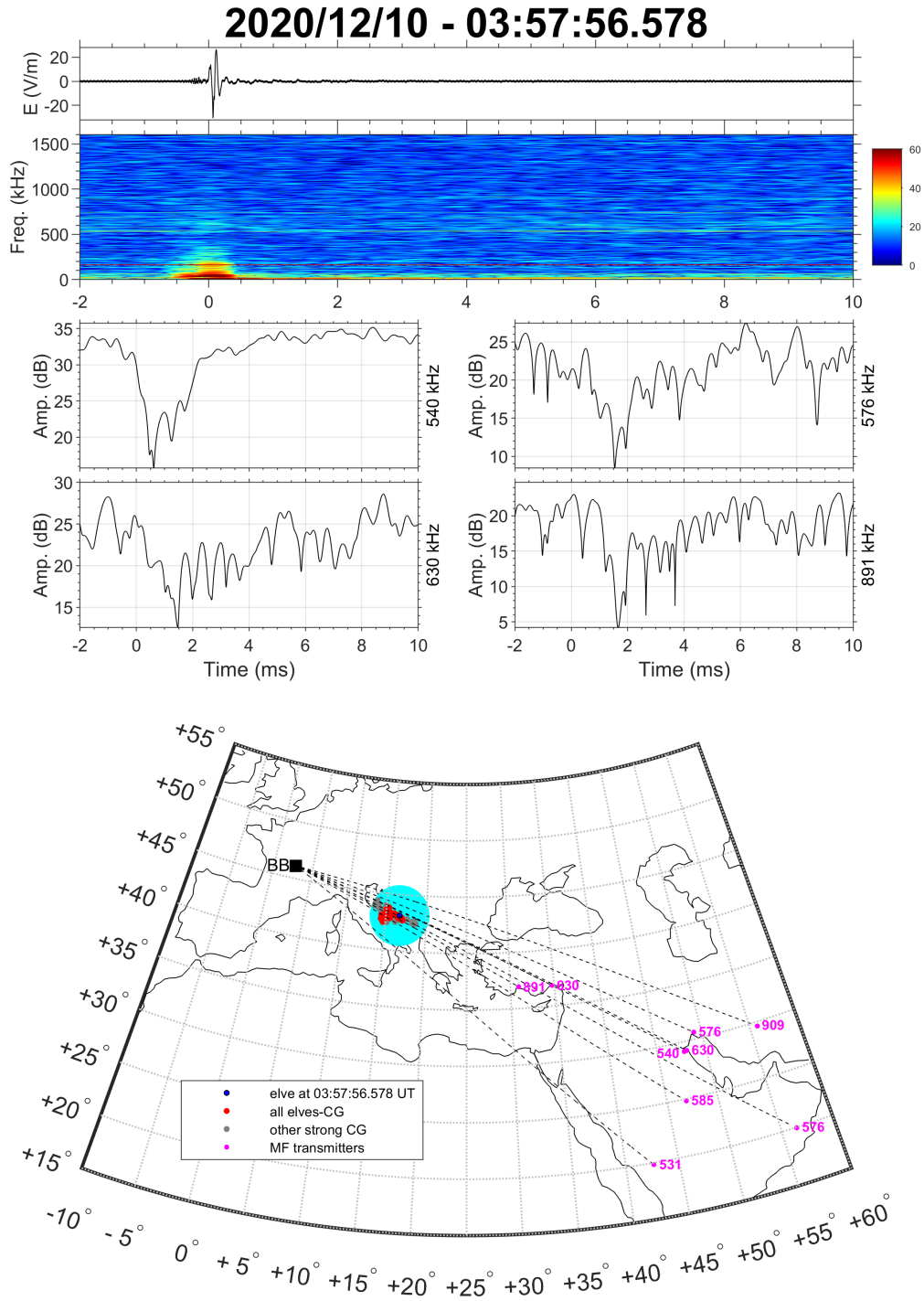


Figure 9. (top) Electric field and associate spectrogram for the elve observed at 03:57:56.578 UTC (shown in Figure 2). (middle): relative amplitude of four transmissions at 540, 576, 630 and 891 kHz (dB). (bottom): map showing the location of the strong CG strokes occurring during the December 9 to 10, 2020 over the Adriatic Sea (grey circles without elves, red ones with elves, the blue circle is for the elve at 03:57:56.578 UT and the light blue disk indicates where the elve is theoretically expanding), magenta dots show the location of transmitters used in this study and the dashed curves are the GCPs of each of these transmitters to the CEA station located in the center of France.

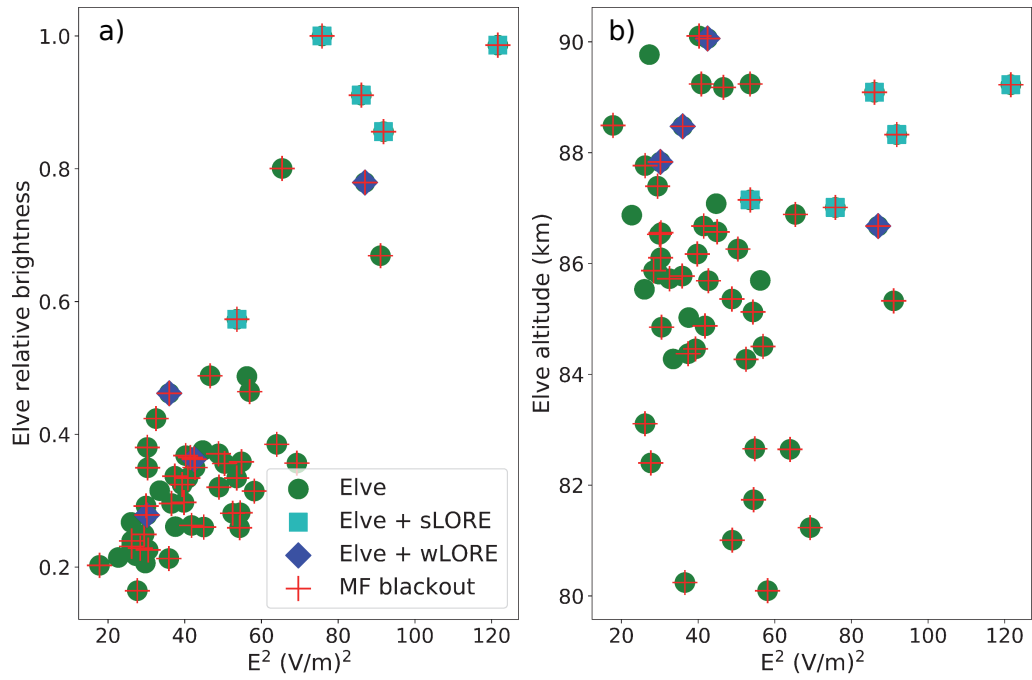


Figure 10. a) Elve relative brightness vs. stroke $P(E^2)$ calculated over 1.5 ms. The elves associated with LOREs and MF blackouts are marked. b) Elve altitude vs. stroke $P(E^2)$ calculated over 1.5 ms. The uncertainty on the altitude is ± 1.7 km.